Full paper/Mémoire

Integrative chemistry portfolio toward designing and tuning vanadium oxide macroscopic fibers sensing and mechanical properties

Nicolas Brun [a], Céline M. Leroy [a], Julien Dexmer [a], Hélène Serier [a], Florent Carn [a,b], Lahire Biette [a], Rénal Backov [a,*]

[a] CNRS UPR 8641, centre de recherche Paul-Pascal, université Bordeaux-I, 115, avenue Albert-Schweitzer, 33600 Pessac, France
[b] CNRS UMR 7057, laboratoire matière et systèmes complexes, université Paris-VII Diderot, bâtiment Condorcet, 10, rue Alice-Domon-et-Léonie-Duquet, 75205 Paris cedex 13, France

Abstract

Under certain synthetic conditions vanadium oxide gels are made of nanoribbons subunits. Due to this textural specificity it is possible to align the ribbons while employing an extrusion process, generating thereby vanadium oxide macroscopic fibers. In this process V_2O_5 gel is extruded through a syringe within a PVA (1% wt) solution rotating beaker. A composite fiber can be then extracted from the beaker. These as-synthesized fibers are bearing outstanding mechanical properties (20 GPa of Young modulus) addressed with transversal flexibility that alloys macroscopic knot formation. Furthermore, they appear to be excellent alcohol sensors, enable to detect 0.1 ppm of ethanol within 16 s at 40 °C, sensitivity being associated with a good selectivity. Subsequently, we were able to tune the fibers' sensing and mechanical properties by varying the shear rate addressed to the vanadium oxide extruded gel. In order to better appreciate the correlation between fibers' porosity, nanoribbons subunits alignment and the addressed properties (mechanical and sensing) we tuned the porosity making the use of latex nanoparticles inclusion followed by their calcinations while varying still the imposed sheer rate during the extrusion. Finally synthesis of hybrid PANI–V_2O_5 allowed reaching enhanced tenacity 12 J g^{-1}, concomitant with a loss of sensitivity. We show that all the parameters involved within the mechanical and sensing performances are acting within a strong partitioning mode rather than a cooperative one. Overall, these iterative synthetic approaches demonstrate once more the importance of the correlation between structures and properties, approaches where the integrative chemistry is appearing, via its versatility, as an essential tool of chemical science to conceive rationally functional architectures bearing enhanced properties. *To cite this article: N. Brun et al., C. R. Chimie 13 (2010).*
© 2009 Académie des sciences. Published by Elsevier Masson SAS. All rights reserved.

Résumé

Sous certaines conditions de synthèse, la texture de gels d'hémipentoxide de vanadium est associée à la présence de rubans nanométriques. Du fait de la forte anisotropie de forme de ces nanorubans il est possible de les aligner au sein d'une fibre macroscopique par un procédé d'extrusion. Dans ce procédé, un gel de V_2O_5 est extrudé par une seringue dans un bécher en rotation contenant une solution d'alcool polyvinylique (PVA) à 1 % massique. Une fibre composite peu alors être extraite du bécher. Les fibres ainsi réalisées possèdent de très bonnes propriétés mécaniques avec un module de Young de l'ordre de 20 GPa et une bonne flexibilité transversale induite par l'anisotropie des briques élémentaires. Ces fibres se sont révélées être de très bons détecteurs de

---

vapeurs d'alcool, capables de détecter 0,1 ppm d'éthanol en 16 secondes à 40 °C, cette sensibilité étant associée à une très bonne sélectivité. Par la suite, nous avons cherché à maîtriser le degré d'alignement des nanorubans de V$_2$O$_5$ au sein des fibres en jouant sur le taux de cisaillement imposé au gel extrudé. Nous avons pu contrôler à la fois leurs propriétés mécaniques et leurs propriétés de senseurs. En vue de mieux appréhender les corrélations entre porosité des fibres, alignements des rubans et les propriétés qui en découlent nous avons ultérieurement fait varier le degré d'alignement des nanorubans en jouant sur le cisaillement imposé sur la goutte extrudée, le taux de porosité, par inclusion et postcalcination de nanoparticules de latex. Cette étude a pu mettre en évidence un fort effet coopératif entre porosité des fibres et alignement des nanorubans sur les propriétés de détections d'alcool et mécaniques. Enfin, la synthèse de fibres hybrides PANI–V$_2$O$_5$/PVA a permis une optimisation de la ténacité de ces fibres, ténacité étant de l'ordre de 12 J/g, associé à une perte de sensibilité. Globalement ces approches itératives mettent en avant une nouvelle fois l'importance des corrélations entre textures et propriétés, approches où la chimie intégrative apparaît par sa versatilité comme un outil essentiel pour concevoir rationnellement des architectures fonctionnelles aux propriétés finales exaltées. ***Pour citer cet article : N. Brun et al., C. R. Chimie 13 (2010).***

1. Introduction

Recently, the new transversal concept of "integrative chemistry" has been postulated as a versatile toolbox, where chemistry, physical chemistry of complex fluids and biology appear as specific items to compose their own synthetic pathway to reach specific multi-scale architectures bearing functionalities acting in registry or not [1]. Integrative Chemistry has been already widely applied by combining general chemistry with foams [2], emulsions [3], lyotropic mesophases [4], biologic polymer [5], three-dimensional colloid opal-like textures [6] and more recently with millifluidic [7]. To the previous set of texturing modes that mostly regard the areas of soft matter, we might combine inorganic polymerization occurring under soft conditions, namely "*chimie douce*" [8]. More precisely, the sol–gel process [9] appears as a candidate of choice to both promote inorganic connectivity while not destroying the templates in use at different length scales. Particularly, vanadium oxide is of strong interest as associated with versatile properties ranging from catalysis to photochromism and so forth [10]. Gels of vanadium oxide can be obtained from sodium metavanadate as inorganic precursor and upon a ion exchange process where the final texture is composed of vanadium oxide nanoribbon subunits bearing strong anisotropy [9b,11] and allows generating an inorganic liquid crystal associated with a nematic character [12].

In the above context, we first took benefit of this textural property to align the ribbon subunits with the use of an extrusion process, generating thus the first macroscopic fibers made of vanadium oxide bearing specific alcohol sensors properties [13], while later on,

by varying the shear rate applied to the extruded gel we were able to tune both the as-synthesized fibers' mechanical and sensing properties [14]. In a third study, by varying the starting latex inclusion contents, the shear rates applied during the extrusion process and by performing a thermal treatment we were able to segregate each parameter involved within the fibers mechanical and sensing properties, as the amount of the organic-insulator counterpart, the degree of vanadium oxide ribbon alignment and the induced porosity reached upon latex removal [15]. Overall, we found that all the parameters described above and involved within the as-synthesized fibers mechanical and sensing properties are acting within a partitive action mode rather than a cooperative one [15], and we concluded that a nice way to promote and enhance both the fiber sensing and mechanical properties would be to generate an extrinsic plasticity associated with an intrinsic enhanced conductivity. Therefore, we recently synthesized the first vanadium oxide polyaniline (PANI) fibers through the same extrusion process, where the vanadium extruded sol is reduced while the aniline contained within the beaker was oxidized into PANI; we coupled for the first time extrusion process with a redox chemical reaction [16]. To reach these new composite fibers, we took inspiration from earlier work [17] that reported the synthesis of hybrid compounds made of conducting polymers intercalated within V$_2$O$_5$ lamellae for the design of positive electrodes for lithium batteries.

This is this overall synthetic pathway, making the use of sol–gel chemistry, extrusion, rheology of complex fluids, latex inclusion and removal, conducting PANI polymers that we would like to propose and discuss

herein, illustrating thereby one specific integrative chemistry [1] incremental approach employed to reach functional materials bearing enhanced properties.

2. Results and discussion

Upon the general process described in details elsewhere [13–16] vanadium oxide macroscopic fibers can be obtained (Fig. 1) through vanadium oxide gel extrusion within a rotating beaker containing dissolved polyvinyl alcohol polymer (PVA) (see the supplementary section for the overall synthetic pathways). We would like first to mention that there is no shear stress applied to the sol within the syringe since the hydrophilic sol does not wet the internal stainless steel surface which is rather hydrophobic, thereby the flux within the syringe is not a ''Poiseuil'' type but rather a ''plug'' one. Thus the shear stress is only addressed when the sol outcoming flow is in contact with the PVA rotating solution (Fig. 1a). At that stage, the PVA and extruded vanadium oxide gel are certainly interacting through hydrogen bonds, beyond being a simple steric effect where PVA defines a matrice trapping the inorganic fibers within. In a second step the as-synthesized fibers can be extracted vertically from the beaker (Fig. 2b and c). Upon drying, we can observe a vanadium oxide fiber's good transversal flexibility that allows knot formation (Fig. 1d).

The vanadium oxide fibers depict also high scale textural anisotropy as revealed by using optical microscopy between cross-polarizer (Fig. 1e) where we can observe that the transmitted light intensity is strongly related to the relative orientation of the fiber toward the polarizers optical axis. This observation reveals a strong axial textural anisotropy within the vanadium oxide fiber core. In fact, it is well known that
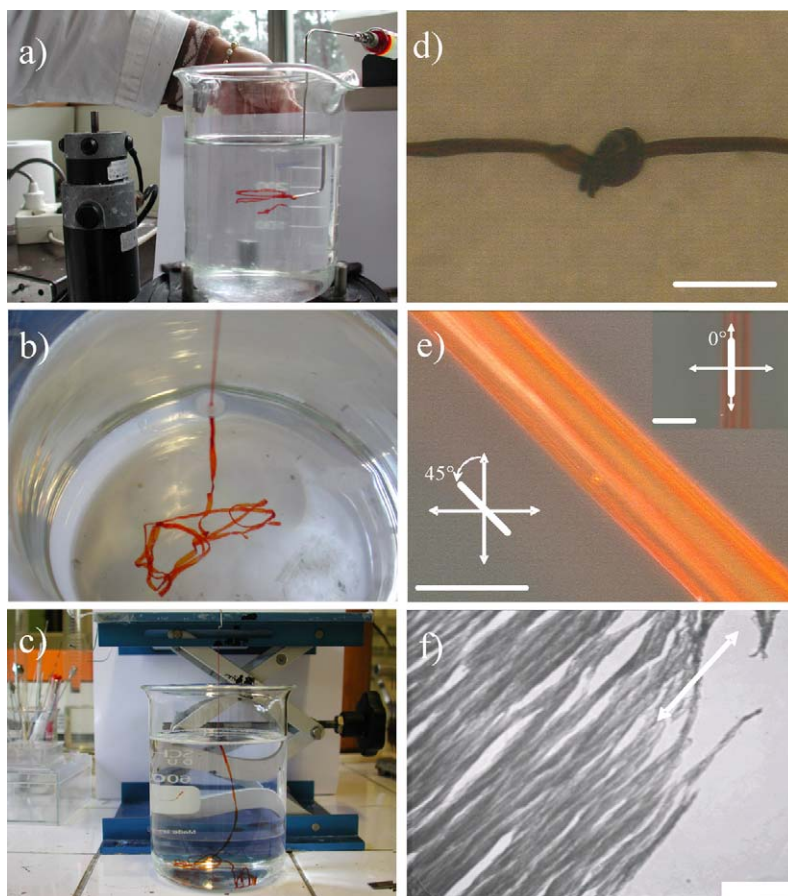

Fig. 1. a: extrusion of the V_2O_5 gel within the rotating beaker bearing the PVA solution; b and c: vertical extraction of the as-synthesized fibers from the beaker; d: vanadium oxide macroscopic fiber transversal flexibility revealed when forming a knot. Scale bars represent 230 µm; e: vanadium oxide fiber observed under cross-polarized microscopy at 45° between analyzer and polarizer (parallel to the analyzer, embedded figure), the scale bare represents 55 µm; f: fiber observed by transmission electron microscopy (TEM), the fibers have been thinned using an electron beam, the scale bar represents 1000 nm.
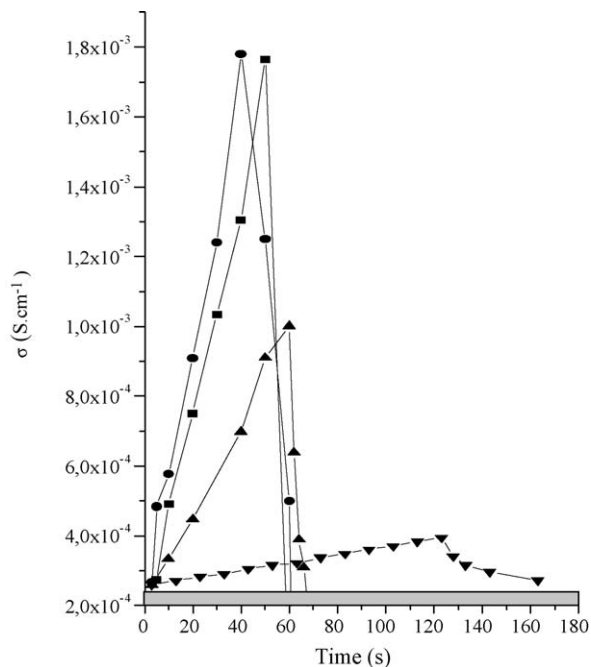
Fig. 2. Typical specific signal shapes with different alcohol vapor sources: ●: ethanol source, ■: methanol source, ▲: propanol source, ▼: pentanol source. The grey part at the bottom of each graph indicates that the multimeter in use is overloading for high resistivity.

vanadium oxide gels used for this study are made of vanadium oxide nanoscopic ribbons that, upon a certain ageing time, allow reaching nematic liquid crystal properties [11,12]. The birefringence depicted with the Fig. 1e demonstrates that preferential orientation has been generated within those fibers. TEM observations reveal that nanoscale ribbon subunits are effectively organized preferentially parallel toward the macroscopic fibers main axis (Fig. 1f). In order to assess longitudinal mechanical properties, traction measurements have been performed over several fibers showing note that they do not possess plastic behavior before they break. When considering longitudinal mechanical properties of the as-synthesized fibers it is obvious to note that they do not possess plastic behavior before they break (Fig. 1, supplemental).

In the elastic regime, at low deformation, we found that the longitudinal Young's modulus varies from 12 to 17 GPa; that corresponds to the values obtained for carbon nanotubes macroscopic fibers obtained through the same extrusion method [18]. This feature demonstrates that the vanadium oxide nanoscopic ribbons, that form the macroscopic fiber, are strongly packed together avoiding thus any longitudinal displacement. Considering both transversal flexibility (Fig. 1d) and the quasi-absence of longitudinal plasticity (Fig. 1, supplemental)

we can deduce that these fibers depict anisotropic mechanical properties. This high scale anisotropic configuration of the nanoscopic vanadium oxide ribbons is certainly induced by the extrusion process where a strong shear is imposed to the gel outcoming flow when injected into the PVA solution. In order to both assess this preferential orientation and avoid any fiber degradation, induced by the ionization beam used for the TEM (Fig. 1f) observation, we also performed SAXS experiments on as-synthesized fibers that reveal an average of $16°$ between the ribbons alignment and the fiber main axis [13].

Considering these fibers as acting as sensors, the first result that should be taken into account is that all the sensing measurements presented below are associated to quantitative conductivity measurements (S cm^{-1}) and not only qualitative (measurement of a resistance in Ohm) as for other works [19]. This point is of great importance, as the sensing capacity can be extrapolated from a specific sensing experimental apparatus to other ones with strong reproducible quantitative values. We can also point out the quite simple experimental set-up mainly induced by the fiber shape, where the fiber is simply stuck on the gold electrodes using silver glue [13,14]. The cells allow measuring the distance of the fiber between the two gold electrodes (L) while their surface diameter having been previously measured using an optical microscope (S). As we can check the system resistance (R) using a multimeter, the conductivity is obvious to be calculated i.e. $\sigma = L/(R \times S)$. We have first checked the as-synthesized sensor responses toward different alcoholic vapor sources. We first showed that conductivity isotherm responses are cycling when the vanadium oxide sensing experimental setup is exposed or extracted subsequently to alcohol vapor source and the increasing–decreasing conductivity turn over is occurring instantaneously. Secondly, we found out that semiconductive time responses are strongly correlated to the alcohol alkyl tail lengths and vary from instantaneous response for methanol and up to 330 s when pentanol is used as alcohol vapor source. This behavior is certainly due to the vapor tension that decreases from methanol to pentanol. Also, both the increase and decrease of conductivity are strongly related to the alcohol nature, resulting in specific signal shape (Fig. 2), those specific signal shapes acting so as a direct signature of the alcohol nature providing thereby specific selectivity. Also, considering Fig. 2, the conductivity value reached for methanol is in the same range as that obtained for ethanol, but those values are decreasing drastically when propanol or pentanol are used as vapor sources. A

conductivity mechanism has been hypothesized elsewhere [19] in terms of surface charge electron-depletion strongly associated to the O–H bonds ionic character. Considering the alcohols used in this study, the donor inducting effect over the oxygen is diluted when going from methanol to pentanol, minimizing thus both the O–H bond ionic character (or basically the acidity) and thus the associated conductivity. Furthermore, and beyond cycling signals and their associated selectivity of shape, it is important to appreciate the sensibility of the vanadium oxide fiber sensing-cells. We found out that a single vanadium oxide fiber allows detecting down to 0.1 ppm within 16 s, detection time that is decreasing to 7 s for 100 ppm, this for a working temperature of 40 °C. It is important to note that the present working temperature, 40 °C, is by far lower when compared to other works where sensing effects over ethanol gas sources were conducted between 150–400 °C [19]. This experiment demonstrates the extremely high sensitivity of the vanadium oxide sensing fibers obtained in this study. Also, those vanadium oxide fiber-made sensing cells are still active after several weeks of experiments.

Overall, with this first study, we have prepared for the first time vanadium oxide macroscopic fibers using an extrusion process, taking benefit of the nanoscopic subunit ribbons' high aspect ratio. Those fibers depict good transversal flexibility and longitudinal mechanical strength associated with a Young's modulus around 15–17 GPa, comparable to fibers made of carbon nanotubes. They are constituted of nanoscopic ribbon subunits associated to a strong preferential orientation parallel to the fibers main axis. Those fibers demonstrate good selectivity as well as strong and fast sensibility toward sensing alcohol vapor, to the limit of 0.1 ppm of ethanol detected within 16 s at 40 °C. Also, due to the vanadium oxide fibers shape that eases the experimental setup, sensing cells are very simple to construct. Furthermore, results are provided in S cm^{-1} and thus they can be now extrapolated from experimental setup to other ones giving rise to absolute quantitative values.

In order to improve the fiber performance when acting as a sensor and addressed with a fine control of their mechanical properties, we performed a full study where the shear rate imposed to the extruded vanadium oxide droplets was the variable in use [14].

2.1. Effects of applied shear rates over the fibers sensing and mechanical properties

The shearing rate $\dot{\gamma}$, associated to the extrusion process, is strongly related to the needle position within the rotating beaker. In this study, we have changed the needle position into the beaker in order to estimate the shearing rate effect over the ribbon subunits alignment within the macroscopic fiber and over the fiber specific properties. Considering the size of the beaker, three positions were used and the shearing rates rose when the extrusion proceeds closer to the beaker outerpart. During all the extrusion processes, the needle is maintained horizontal and tangentially to the beaker rotation, at the same depth (around 1 cm) while keeping the beaker rotating speed constant. With the different positions are associated specific PVA solution linear speeds (V_b). Considering the vanadium oxide sol extrusion speed (V_e) and (d) the needle diameter (400 μm), we can estimate a shear rate ($\dot{\gamma}$) associated to each position, taking into account the Eq. (1) [20]:

$$\dot{\gamma} = \frac{dV}{dx} \approx \frac{(V_b - V_e)}{(d/2)} \tag{1}$$

Thus the three different needle positions from the inner to the outer part of the beaker correspond to respectively the three different shear rates $\dot{\gamma}$ equal to $-158\ \mathrm{s}^{-1}$, $100\ \mathrm{s}^{-1}$ and $235\ \mathrm{s}^{-1}$. The negative shear strength, associated to the needle position closer to the beaker center, indicates that the speed of the vanadium oxide outcoming flow is higher than the rotating beaker one. In this case, the size of the vanadium oxide extruded flow should increase when compared to the two other applied shear strengths, and by this way should lead to larger fiber diameters. By varying the shear rate ($\dot{\gamma}$) imposed during the extrusion process it is possible to tune the as-synthesized vanadium oxide fiber macroscopic morphologies (Fig. 3a–f) as well as the ribbon subunits preferential alignments (Fig. 3 g,h,j) where we can see that the fiber birefringence increases with the strength of the applied shear rate. Beyond this contemplative issue, it is important to estimate the average tilt angle of the nanoribbons toward the macroscopic fiber main axis, providing more quantitative results. We thus performed small angle X-ray scattering (SAXS) experiments. A representative SAXS pattern of a fiber shows an anisotropic diffuse spot around the beam trap [14] associated with a vanadium oxide ribbons' main title angles that vary from 17° to 28° as the strength of the applied shear rate is decreasing. As previously observed [13], the scattered intensity I of this diffuse spot regularly decreases with the scattering vector modulus q as q^{-2} [21], which corresponds to the form factor of plate-like ribbons. These fiber's mechanical properties should be strongly related with the specific alignment of the nanoscopic ribbon subunits.
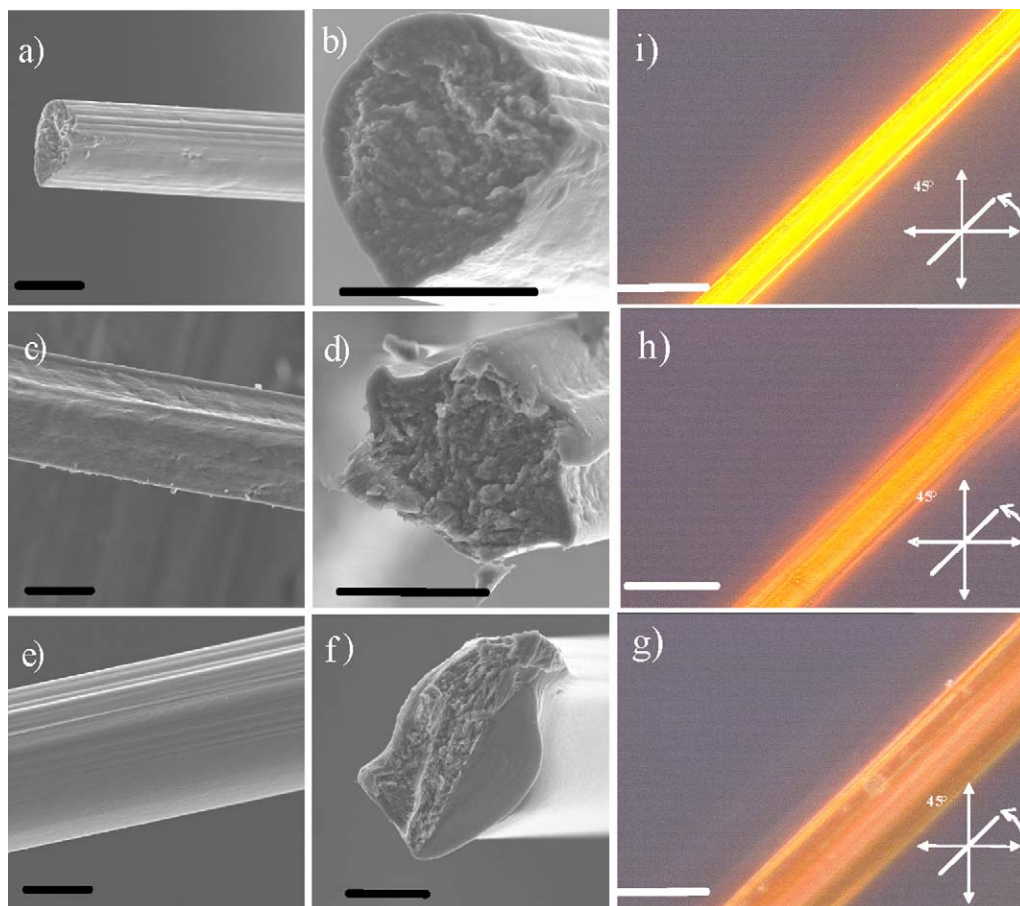
Fig. 3. SEM observations performed on vanadium oxide fibers. a and b: fibers synthesized upon a shearing rate $\dot{\gamma}$ equals to 235 s^{-1}; c and d: fibers synthesized upon a shearing rate of $\dot{\gamma}$ equals to 100 s^{-1}; e and f: fibers generated with the highest shearing rate $\dot{\gamma}$ equal to −158 s^{-1}. The scale bars represent 20 μm. Vanadium oxide fibers observed through cross-polarized microscopy at 45° between the analyzer and polarizer: g: $\dot{\gamma}$ equals to 235 s^{-1}; h: $\dot{\gamma}$ equals to 100 s^{-1}; i: $\dot{\gamma}$ equals to −158 s^{-1}. The scale bar represents 50 μm.

For each employed shear rate, several mechanical measurements were carried out in order to calculate average mechanical characteristics of each kind of fibers (Fig. 4a). As observed on Fig. 4a, the fibers possess a weak plastic behavior before they break; this plastic regime is decreasing when the shear rate strength is increasing. Considering the fact that an increase of the shear rate is associated with a better alignment of the nanoribbon subunits parallel toward the fiber main axis, the feature observed here is expected. When considering the Young's modulus (E), there is a strong enhancement when increasing the shear rate varying from 13 GPa for the lower shear rate to 22 GPa for the higher one. Here again, as the nanoribbon subunits are more aligned when increasing the shear rate, both the Young's modulus and rigidity (σ) increase. Also we have to acknowledge the fact that the Young modulus of those vanadium oxide fibers appears to be in the same range as the best ones obtained for fibers made of carbon nanotubes [18].

With Fig. 4b, we can observe that the sensitivity is enhanced (lower detection times) when the fibers are promoted using the higher shear rate. The following two parameters, ribbon alignment and textural mesoporosity, that should play a crucial role toward the sensing effect, are antagonistic, i.e. when the ribbon alignment, or stacking, is increasing then the textural porosity should decrease. If we consider the fact that, whatever the shear rate imposed during the extrusion process, final fibers are, at most, poorly mesoporous [13], the main factor that can explain the sensitivity variation with the shear rate applied is only the ribbon alignment. In that case, we can state that the nanoribbons' better alignment, obtained through the higher shear rate, is favoring the electron-depletion phenomenon and thus the fiber sensitivity [19]. On the other hand, as there is
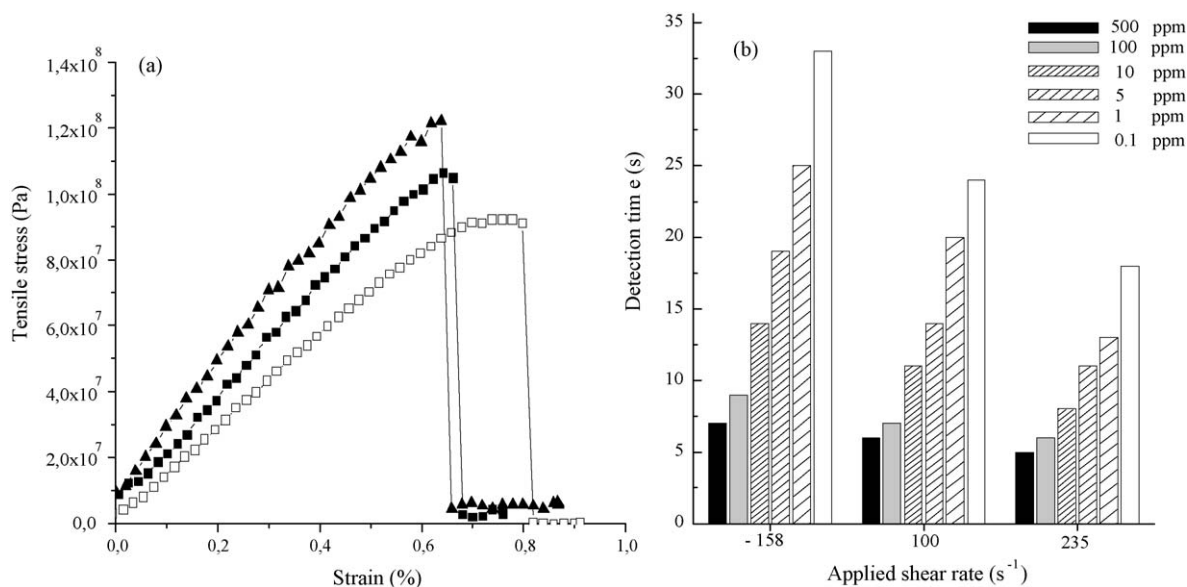
Fig. 4. a: vanadium oxide fibers mechanical properties for each shearing rate. Measurements were performed at a strain rate of 0,3 mm/min. $\square$: $\dot{\gamma}$ equals to -158 s^{-1}, $\blacksquare$: $\dot{\gamma}$ equals 100 s^{-1}, $\blacktriangle$: $\dot{\gamma}$ equals 235 s^{-1}; b: histogram that depicts the vanadium oxide fibers ethanol sensitivities at 40 °C. The experimental set-up is placed above a beaker containing ethanol whose concentration varies from 500 ppm down to 0.1 ppm. Ethanol has been diluted into THF because THF does not promote effect over the conductivity cell. The provided results have been obtained for a single vanadium oxide fiber.

no porosity, once the vanadium oxide external surface has been reduced through alcohol oxidation, the conductivity starts to decrease as the native V^{4+} species are acting as hole potentials for the electron, minimizing thereby the conductivity; the fibers' thermodynamic stability was not very high [14].

We have demonstrated the nanoscopic ribbon subunits alignment, tuned via the shear rate applied during the extrusion process, appears as a good tool to tune both the as-synthesized fibers final mechanical and sensing properties, but the thermodynamic stability when sensing needed to be upgraded.

The next work was dedicated to enhance the fibers' mesoporosity, using adequate scarified latex nanoparticles, as well as promoting vanadium oxide crystallizations through thermal treatment. We thereby intended to evaluate if the ribbons specific alignment, the associated mesoporosity and the V_2O_5 degree of crystalline character are involved either in a cooperative or partitioning fashion toward tuning the final fibers sensitivity [15].

2.2. Effects of combining the applied shear rates and the latex inclusion contents over the fiber's sensing and mechanical properties

As previously demonstrated, by varying the shear rate (γ) imposed during the extrusion process it is

possible tuning the as-synthesized vanadium oxide fiber macroscopic morphologies as well as the ribbon subunits preferential alignments (Fig. 5a and b). We can notice a decrease in the brightness as the latex concentration is increased, while maintaining the shear rate constant. This observation by itself is not sufficient to state that the ribbons' preferential orientation is disturbed by the latex nanoparticle adjunction, as an increase of the latex concentration will also diminish light transmission during the optical microscopy experiments (transmission mode used for the cross-polarized optical experiments). We thus make the use of SAXS experiments to better qualify the effect (Fig. 5c). As previously reported [13,14], an anisotropic X-ray pattern is observed in the small angles region revealing a preferred orientation of the V_2O_5 ribbons along the fiber axis. Again, at the microscopic length scale, the as-synthesized fibers depict the same microstructure as vanadium oxide xerogels V_2O_5. 1.8 H_2O [13,14,22]. As mentioned before [13,14], the intrinsic one-dimensional nature of the as-synthesized vanadium oxide fibers allows generating sensing cells with a certain degree of simplicity.

We previously demonstrated that PVA/vanadium oxide fibers were able to sense 0.1 ppm of ethanol within 16 s at 40 °C, with good cycling properties and selectivity toward diverse alcohol [13,14]. The goal of this study is first to search for higher sensitivity and high
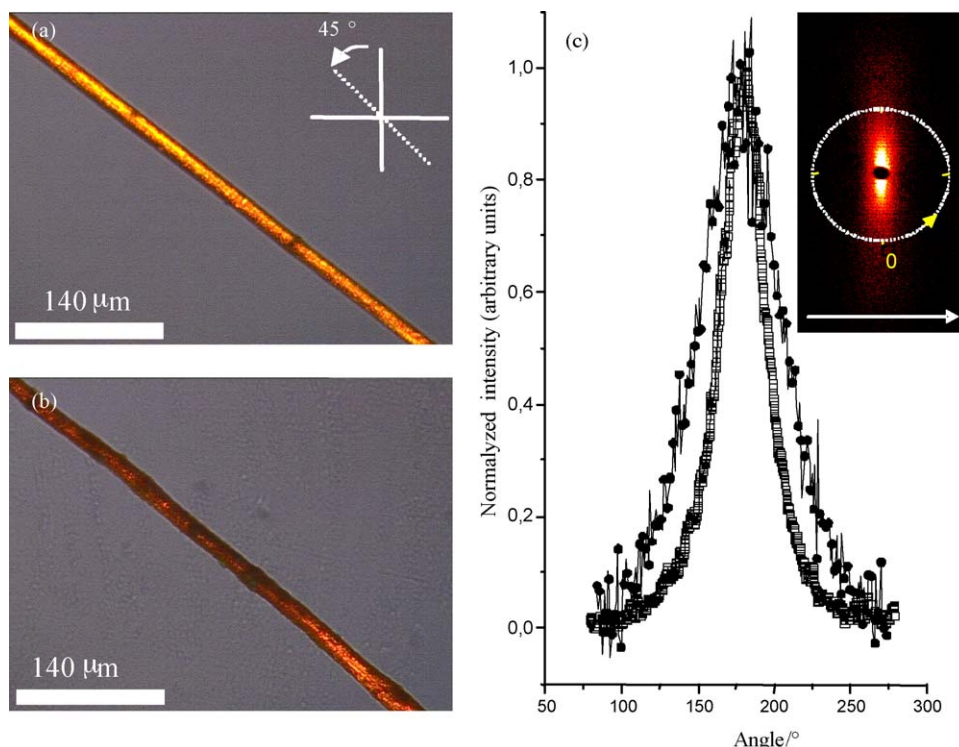
Fig. 5. a–b: fibers observed through cross-polarized optical microscopy: a: 10% latex and $\gamma = 235$ s^{-1}; b: 60% latex and $\gamma = 235$ s^{-1}; c: SAXS spectra, □: 0% latex and $\gamma = 235$ s^{-1}, ●: 60% latex and $\gamma = 235$ s^{-1} (the embedded figure depicts the anisotropic diffused pot with the fiber main axis being positioned parallel to the white arrow).

thermodynamic stability while sensing. Beyond, the sensing and stability results will be discussed in terms of the nanoribbons alignments, the latex contents and the effect of their removal. Results considering the fiber sensibilities are provided for calcined ones on Fig. 6. The effect of latex concentration over the sensing properties was rather weak, with a soft trend that intends to show that an increase in the latex content allows optimizing the sensing properties [15]. For instance, at 42 °C the sensing time to detect 0.1 ppm of ethanol decreases from 11 to 9 s. Obviously, we are in the limit of the error (1.5 s) for the time detection and considering this issue, we would say that the effect of the latex contents, at a constant shear rate, cannot be detected with the apparatus in use but stay, overall, within the same range when compared with vanadium oxide fibers free of latex particles [13,14]. Also, The effect of both latex content and applied shear rate during the extrusion were very weak, with a soft tendency of increasing the sensing properties as the applied shear rate increases. This fact is indeed expected as, increasing the shear rate allows a better alignment of the nanoribbon subunits, a feature that eases the generation of conductor domains taking into account the surface conducting electron-depletion scenario [19].

Considering that the nanoribbons are statistically connected together, via hydrogen bonds within the macroscopic fibers, then electrons can pass through the entire fiber which becomes an electronic conductor. The better alignment of the nanoribbon subunits will provide the higher sensitivity. Considering the Fig. 6, it is obvious that fiber sensibility is increased when removing most of the organic content.

In fact, both PVA and latex are insulator components and their removal will thus enhance the fiber intrinsic conductivity. The detection time, for calcined fibers, has been generally divided per three; specifically 0.1 ppm of ethanol at 42 °C can now be detected within 3 to 5 s (Fig. 6). Again, the effect of porosity, emerging from the removal of the starting latex and PVA contents (Fig. 6a) and the effect of the applied shear rate (Fig. 6b) over the detection time, are very hard to analyze as again the difference observed are basically within the limit of the error (1.5 s) for the time detection.

Also, we demonstrated that the fibers are much more stable under alcoholic vapor, particularly the stability increases as the induced porosity increases [15], the fibers that depict the higher stability being the ones emerging from the 60% latex content removal. We
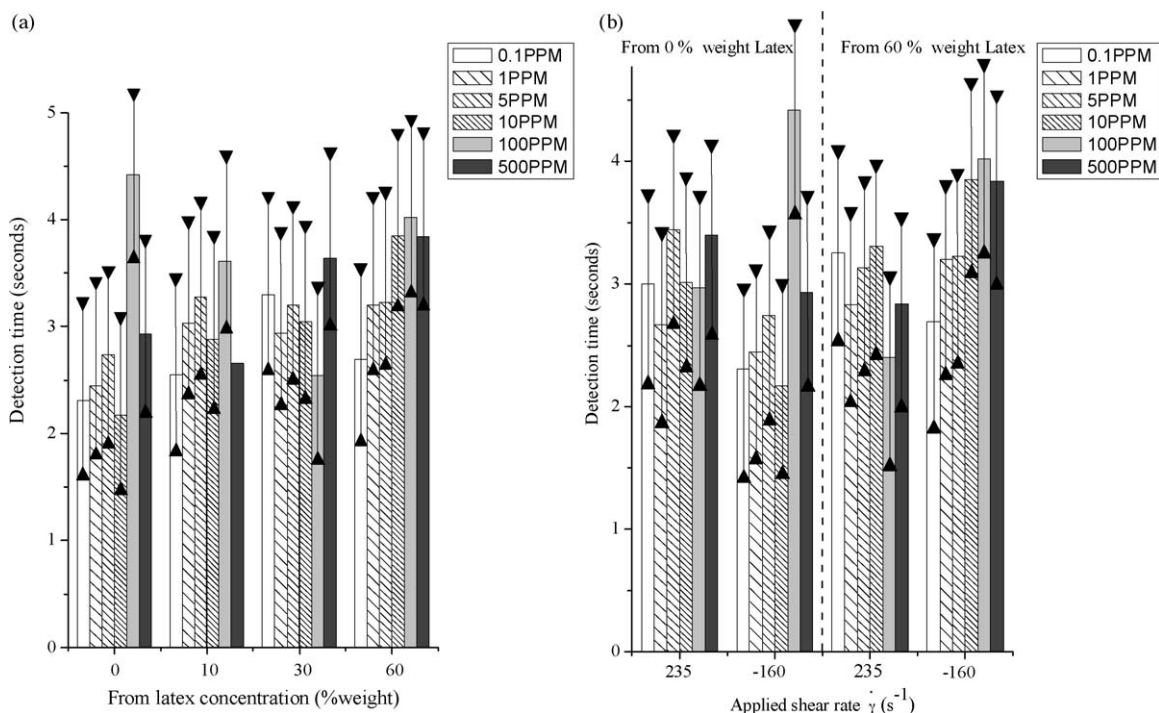
Fig. 6. Histograms that depict porous inorganic V$_2$O$_5$ fiber sensitivities at 42 °C for. The experimental set-up is placed above a beaker containing ethanol whose concentration varies from 500 ppm down to 0.1 ppm. Ethanol has been diluted into THF because THF does not promote effect over the conductivity cell. The provided results have been obtained for a single vanadium oxide fiber. a: effect of latex contents at 235 S^{-1}; b: effects of latex contents and applied shear rate. The sensitivity measurements are made by determining the point at which the multimeter in use is no longer overloading, i.e., when it is able to measure a finite resistance above 180 Mç.

found here the same trend concerning the effect of the shear rate over the thermodynamic stability than the one observed for fibers free of latex particles [14], when the shear rate increases the fibers stability decreases. As a direct consequence the fibers promoted through the lower shear rate and from the higher latex content are associated with the higher stability, because we just optimize the alcohol diffusion within the fibers core and thus the number of sublayers electronic pathways that allow maintaining the conductivity at a maximal value. This particular study renders valid the scenario where sublayers can relay the conductivity process when the upper layer V^{5+} sites are completely reduced [14].

With this study, composite vanadium oxide/PVA/latex macroscopic fibers have been generated by using an extrusion process. Specifically, inorganic vanadium oxide fibers enable to detect 0.1 ppm of ethanol within 3 to 5 s at 42 °C have been obtained through the organic counterparts removal (thermal treatment), which is certainly one of the highest sensibility never reached to date concerning the alcohol sensors. More importantly, by varying the starting latex inclusion contents, the shear rates applied during the extrusion process and with the final appliance of a thermal treatment we were

able to segregate each parameter involved within the mechanical and sensing properties associated with these as-synthesized fibers, i.e. the amount of the organic-insulator counterpart, the degree of vanadium oxide ribbons alignment and the induced porosity reached upon latex removal. Overall, we found that all the parameters described above and involved within the as-synthesized fibers mechanical and sensing properties are acting within a partitive action mode rather than a cooperative one.

On the other hand, the mechanical properties of the porous inorganic vanadium oxide fibers were very weak. At that stage we concluded that a nice way to promote and enhance both the fiber sensing and mechanical properties would be to ''generate an extrinsic plasticity associated with an intrinsic enhanced conductivity''. This work [16] is summarized in the next section.

2.3. Effects of generating PANI/PVA/V$_2$O$_5$ nanocomposite fibers over sensing and mechanical properties

We recently synthesized the first vanadium oxide polyaniline (PANI) fibers through the extrusion process
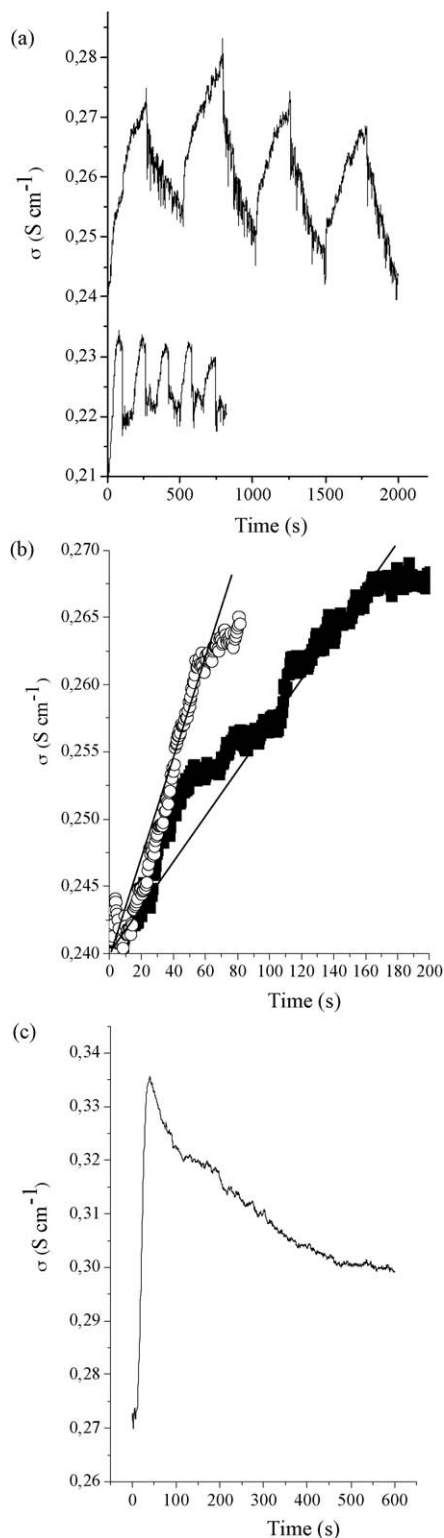
described, where the vanadium extruded sol is reduced while the aniline contained within the beaker is oxidized into PANI; we coupled for the first time the extrusion process with a redox chemical reaction [16]. To reach these new composite fibers, we took inspiration from earlier work [17] that reported the synthesis of hybrid compounds made of conducting polymers intercalated within V_2O_5 lamellae for the design of positive electrodes for lithium batteries. As claimed before, the intrinsic fiber shape is offering the ability to construct conductive cells with high degree of simplicity [13]. Also, the fiber section as well as the nanoribbons preferential orientation (and associated packing density) can be tuned playing with the applied shear rate applied during the extrusion process [14]. We previously demonstrated that the higher alignment of the nanoribbons subunits will permit to get the higher sensitivity [13–15]. The fiber section can be measured using either optical microscopy or SEM (Fig. 3b,d,f) and for a known fiber length the sensing properties can be now quantitatively estimated with a conductivity measurement. The overall sensing properties are shown on Fig. 7.

First, considering the Fig. 7a we can notice that the fibers are cycling. This feature is expected as already observed with the first vanadium oxide fibers generated using the extrusion process mentioned inhere [13–15]. The important issue, beyond cycling, is that the responses toward ethanol or butanol vapors source are not the same, as observed when considering the slope of the increasing conductivities under alcoholic vapor (Fig. 7b), for the same reasons than the ones described above in the text. This particularity demonstrates the new PVA/PANI–V_2O_5 oxide fibers are still selective toward sensing different alcohol vapors, when compared with our previous works [16,18].

On the other hand, when sensing, we can notice here that the increase of conductivity is low, varying only the second decimal placed on the conductivity scale. This was not the case with previous work [13–15] where the sensing performance took place with one or two orders of magnitude over the conductivity measurements. Herein, the PVA/PANI–V_2O_5 fibers are bearing a bimodal conductivity due to the p-doped conducting polyaniline inserted into an n-doped vanadium oxide host matrix. As a direct consequence, the intrinsic starting fibers' conductivity (without alcohol vapors) is

Fig. 7. Sensing properties of PVA/PANI–V_2O_5 oxide fibers. a: fibers cycling abilities upon butanol (top) and methanol (down) alcoholic vapors; b: zoom over the increasing conductivities when fibers are positioned above alcoholic vapor, ○: ethanol, ■: butanol (the butanol curve has been translated down to help comparing the curves slope, plain line); c: evolution with time of the vanadium oxide fibers conductivity profiles at 42 °C when placed above a beaker containing pure ethanol. The results have always been obtained for a single vanadium oxide fiber constituting the conductive cell.

higher than the PVA/V_2O_5 and the pure inorganic ones. As ascribed with ESR quantitative measurements, the redox intercalation of aniline is associated with a strong reduction of the V^{5+} species into V^{4+} ones. Considering this issue, and as the vanadium oxide fibers' sensing property is based on the oxidation of alcohol into aldehyde upon reduction of V^{5+} species into V^{4+} ones [19,15], the potential of V^{5+} species of being reduced through alcohol vapors is thereby strongly minimized, diminishing thus both the sensitivity and the amplitude of the conductivity's increase when sensing alcohol vapors. Beyond cycling and selectivity properties, it is important to check for the fiber thermodynamic stability when exposed for a long time above alcohol vapors, the result is proposed on Fig. 7c. We can observe a first conductivity increase to a maximum, followed by an abrupt loss of conductivity. As previously observed [14,15], this loss of conductivity is associated with a fiber color change from red to green, meaning that V^{5+} species are reduced to V^{4+}, creating thus a potential hole that diminishes the conductivity. When comparing this results with previous ones [16–18], especially with inorganic fibers bearing nanoporosity [15], the thermo-dynamic stability of the fibers presented herein has been lowered, mainly for two reasons. First, due to the aniline/V_2O_5 redox reaction, the concentration of V^{4+} species has been enhanced. Secondly these fibers do not possess any induced porosity, thus when all the V^{5+} present at the fiber outerpart is completely reduced, the surface conductivity is drastically damaged, without any sublayer conductive domains compensation that have been shown to be induced by promoting nanoporosity [15]. Also, considering these fibers sensitivity, they are able to detect 5 ppm of ethanol within 3 to 5 s, with 35 s to reach 90% of the maximal conductivity value. This sensibility at 42 °C is lower when compared with pure inorganic nanoporous vanadium oxide fibers where, for instance, the best sensibility allows sensing down to 0.1 ppm of ethanol within 3–5 s at 42 °C [15]. On the other hand, we have to bear in mind that the pure inorganic nanoporous fibers were extremely fragile mechanically which is not the case with the fibers presented here, as discussed below in the text.

Considering the mechanical properties we can see the fiber behavior through the adding of PANI is totally different (Fig. 8).

The PVA/vanadium oxide fibers possess both a short elastic regime associated without any plastic regime. As a direct consequence, the Young modulus is quite high 22 GPa with a weak strain before breaking. When introducing PANI through the generation of the new
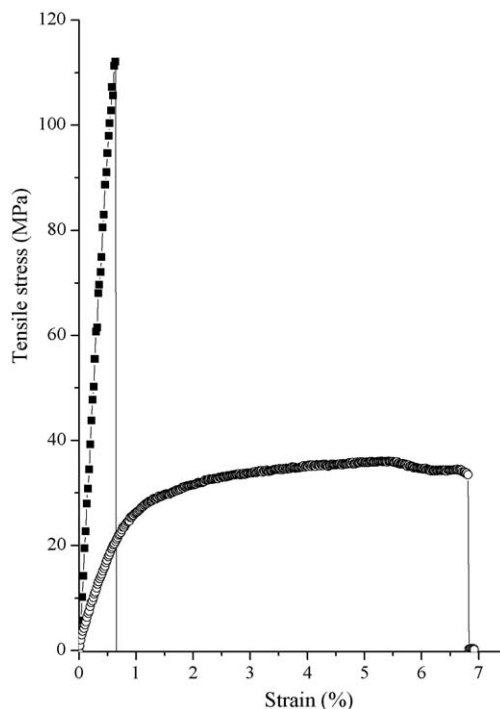

Fig. 8. Fiber mechanical properties. Measurements were performed at a strain rate of 0.3. ■: PVA/V_2O_5 fibers, ○: PVA/PANI–V_2O_5 fibers. The fibers were generated using the same shear rate of 235 s^{-1}.

PVA/PANI–V_2O_5 fibers we can observe on Fig. 8 that the toughness, which is represented at first glance by the surface area under the traction curves, is tremendously increased. The PVA/PANI–V_2O_5 traction curve is bearing a strong plastic regime allowing a strain under traction of around 7%. This feature allows reaching a toughness of 12 J g^{-1}, six times higher than fibers obtained without PANI [16]. When comparing the PVA/PANI–V_2O_5 fibers' toughness with inorganic nanopor-ous fibers, the toughness value has been increased by more than 120 times. On the other hand, as the direct consequence of the enhanced toughness the Young modulus is decreasing to 3.4 GPa. The enhanced toughness bearing by the PVA/PANI–V_2O_5 fibers relies certainly be on the fact that PANI is disrupting the hydrogen bounds between PVA and surfaced V–OH pending groups. This effect optimizes the ability of the nanoribbons subunits to stack–slip on each others while minimizing the obtained Young modulus on the other hand.

For the first time, PVA/PANI–V_2O_5 composites have been generated bearing organization at the mesoscopic and macroscopic length scales as obtained through a redox extrusion process. Also, considering the extrusion process itself, this is certainly the first time that a redox reaction is addressed while performing an extrusion

process. These new PVA/PANI–V$_2$O$_5$ fibers are cycling when still sensing alcoholic vapors while offering a good selectivity. The addressed sensitivity allows sensing 5 ppm of ethanol within 3–5 s at 42 °C, which is lower to that obtained with both composite PVA/V$_2$O$_5$ and inorganic nanoporous vanadium oxide fibers, but higher still than highest results observed for nonfiber-based materials [19]. When sensing, we noticed here that the increase in conductivity is low, varying only the second decimal placed on the conductivity scale. This was not the case with previous work [13–15] where the sensing performance took place with 1 or 2 orders of magnitude over the conductivity measurements. Herein, the PVA/PANI–V$_2$O$_5$ fibers are bearing a bimodal conductivity due to the p-doped conducting polyaniline inserted into an n-doped vanadium oxide host matrix. As a direct consequence, the intrinsic starting fibers' conductivity (without alcohol vapors) is higher than the PVA/V$_2$O$_5$ and the pure inorganic ones. As ascribed with ESR quantitative measurements [16], the redox intercalation of aniline is associated with a strong reduction of the V^{5+} species into V^{4+} ones. Considering this issue, and as the vanadium oxide fibers' sensing property is based on the oxidation of alcohol into aldehyde upon reduction of V^{5+} species into V^{4+} ones,[19] the potential of V^{5+} species of being reduced through alcohol vapors is thereby strongly minimized, diminishing thus both the sensitivity and the amplitude of the conductivity's increase when sensing alcohol vapors. On the other hand, the as-synthesized PVA/PANI–V$_2$O$_5$ macroscopic fibers possess a toughness of 12 J g^{-1}, value six times higher when compared with PVA/V$_2$O$_5$ fibers [13,14] and a factor higher than 120 when compared with nanoporous inorganic fibers [15].

Overall, the use of a redox reaction to promote new PVA/PANI–V$_2$O$_5$ fibers allows a gain of toughness and fibers' intrinsic conductivity but a loss of sensitivity, meaning again that the parameters involved within the fibers' sensing and mechanical properties are acting in a strong partitioning mode rather than a cooperative one.

3. Conclusion

Under certain synthetic conditions vanadium oxide gels are made of nanoribbon subunits. Due to this textural specificity it is possible to align the ribbons while employing an extrusion process, generating thereby vanadium oxide macroscopic fibers. In this process V$_2$O$_5$ gel is extruded through a syringe into a PVA (1% wt) solution rotating beaker. A composite fiber can be then extracted from the beaker. These as-synthesized fibers are bearing outstanding mechanical properties (20 Gpa Young modulus) addressed with transversal flexibility that allows macroscopic knots formation. Furthermore they appear to be excellent alcohol sensors, enable to detect 0.1 ppm of ethanol within 16 s at 40 °C, sensitivity being associated with a good selectivity. Subsequently, we were able to tune the fibers' sensing and mechanical properties by varying the shear rate addressed to the vanadium oxide extruded gel. In order to better appreciate the correlation between fibers' porosity, nanoribbons subunits alignment and the addressed properties (mechanical and sensing) we tuned the porosity making the use of latex nanoparticles inclusion followed by their calcinations while varying still the imposed sheer rate during the extrusion. Finally, synthesis of hybrid PANI–V$_2$O$_5$ allowed reaching enhanced tenacity 12 J g^{-1}, concomitant with a loss of sensitivity. We show that all the parameters involved within the mechanical and sensing performances are acting within a strong partitioning mode rather than a cooperative one. Overall, these iterative synthetic approaches demonstrate once more the importance of the correlation between structures and properties, approaches where the integrative chemistry is appearing, via its versatility, as an essential tool of chemical science to conceive rationally functional architectures bearing enhanced properties.

Appendix A. Supplementary material

Additional material (Fig. S1, S2) that supplements the online version of this article is available at: http://www.sciencedirect.com and doi:10.1016/j.crci.2009.01.007.

References

[1] (a) R. Backov, Soft Mater. 2 (2006) 452 ;
    (b) E. Prouzet, Z. Khani, M. Bertrand, M. Tokumoto, V. Gyuot-Ferreol, J.-F. Tranchant, Microporous Mesoporous Mater. 96 (2006) 369 ;
    (c) C. Sanchez, C. Boissière, D. Grosso, C. Laberty, L. Nicole, Chem. Mater. 3 (2008) 682 ;
    (d) E. Prouzet, S. Ravaine, C. Sanchez, R. Backov, New J. Chem. 32 (2008) 1284.
[2] (a) F. Carn, A. Colin, M.-F. Achard, H. Deleuze, R. Backov, Adv. Mater. 16 (2004) 140 ;
    (b) F. Carn, A. Colin, M.-F. Achard, H. Deleuze, C. Sanchez, R. Backov, Adv. Mater. 17 (2005) 62 ;
    (c) F. Carn, N. Steunou, J. Livage, A. Colin, R. Backov, Chem. Mater. 17 (2005) 644.
[3] (a) A. Imhof, D.J. Pine, Nature 389 (1997) 948 ;
    (b) S. Schacht, Q. Huo, I.G. Voigt-Martin, G.D. Stucky, F. Schüth, Science 273 (1996) 768 ;
    (c) F. Carn, A. Colin, M.-F. Achard, E. Sellier, M. Birot, H.

Deleuze, R.J. Backov, Mater. Chem. 14 (2004) 1370 ;
(d) G. Fornasieri, S. Badaire, R. Backov, O. Mondain-Monval, C. Zakri, P. Poulin, Adv. Mater. 16 (2004) 1094 ;
(e) S. Ungureanu, M. Birot, G. Laurent, H. Deleuze, O. Babot, B. Julián-López, M.-F. Achard, M.I. Popa, C. Sanchez, R. Backov, Chem. Mater. 19 (2007) 5786.

[4] J.H. Jung, Y. Yoshiyuki, S. Shinkai, Angew. Chem. Int. ed 39 (2000) 1862.

[5] S.R. Hall, H. Bolger, S. Mann, Chem. Commun. (2003) 2784.

[6] D. Wang, R.A. Caruso, F. Caruso, Chem. Mater. 13 (2001) 364.

[7] (a) M. Tachibana, W. Engl, P. Panizza, H. Deleuze, S. Lecommandoux, H. Ushiki, R. Backov, Chem. Eng. Process : Process Intensification 47 (2008) 1323 ;
(b) W. Engl, M. Tachibana, P. Panizza, R. Backov, Int. J. Mult. Flow 33 (2007) 897 ;
(c) P. Panizza, W. Engl, C. Hany, R. Backov, Col. Surf. A: Phys. Eng. Aspects 312 (2008) 24 ;
(d) W. Engl, R. Backov, P. Panizza, Current Opinion Col. § Int. Science 13 (2008) 206.

[8] J. Livage, New J. Chem. 25 (2001) 1.

[9] (a) C.J. Brinker, G.W. Scherer, Sol–Gel Science: the Physics and Chemistry of Sol–Gel Processing, Academic Press, San Diego, 1990 ;
(b) J. Livage, Chem. Mater. 3 (1991) 578.

[10] (a) L.C.W. Baker, D.C. Glick, Chem. Rev. 98 (1998) 3 ;
(b) P.J. Hagrman, R.C.O. Finn, J. Zubieta, J. Solid State Sci. 3 (2001) 745.

[11] (a) H.Z. Zöcher, Anorg. Allg. Chem. 147 (1925) 91 ;
(b) J. Lemerle, L. Nejem, J. Lefebvre, J. Inorg. Nucl. Chem. 42 (1980) 77.

[12] (a) O. Pelletier, P. Davidson, C. Bourgaux, J. Livage, Progr. Colloid. Polym. Sci. 112 (1999) 121 ;
(b) X. Commeinhes, P. Davidson, C. Bourgaux, J. Livage, Adv. Mater. 9 (1997) 900.

[13] L. Biette, F. Carn, M. Maugey, M.-F. Achard, J. Maquet, N. Steunou, J. Livage, H. Serier, R. Backov, Adv. Mater. 17 (2005) 2970.

[14] H. Serier, M.-F. Achard, N. Steunou, J. Maquet, J. Livage, C.M. Leroy, O. Babot, R. Backov, Adv. Funct. Mater. 16 (2006) 1745.

[15] C.M. Leroy, M.-F. Achard, O. Babot, N. Steunou, P. Massé, J. Livage, L. Binet, N. Brun, R. Backov, Chem. Mater. 19 (2007) 3988.

[16] J. Dexmer, C.M. Leroy, L. Binet, N. Brun, C. Coulon, J. Maquet, P. Launois, N. Steunou, J. Livage, R. Backov, Chem. Mater. 20 (2008) 5541.

[17] (a) M.G. Kanatzidis, C.-G. Wu, H.O. Marcy, C.R. Kannewurf, J. Am. Chem. Soc. 111 (1989) 4139 ;
(b) C.-G. Wu, D.C. DeGroot, H.O. Marcy, J.L. Schindler, C.R. Kannewurf, Y.-J. Liu, W. Hirpo, M.G. Kanatzidis, Chem. Mater. 8 (1996) 1992 ;
(c) F. Leroux, B.E. Koene, L.F. Nazar, J. Electrochem. Soc. 143 (1996) L181 ;
(d) P. Gomez-Romero, Adv. Mater. 13 (2001) 163 ;
(e) O.Y. Posudievsky, S.A. Biskulova, V.D. Pokhodenko, J. Mater. Chem. 14 (2004) 1419.

[18] B. Vigolo, A. Pénicaud, C. Coulon, C. Sauder, R. Paillet, C. Journet, P. Bernier, P. Poulin, Science 290 (2000) 1331.

[19] (a) G. Micocci, A. Serra, A. Tepore, S. Capone, R. Rella, P. Siciliano, J. Vac. Sci.Technol. A 15 (1997) 34 ;
(b) J. Liu, X. Wang, Q. Peng, Y. Li, Adv. Mater. 17 (2005) 764.

[20] R.G. Larson, The structure and rheology of complex fluids, Oxford University Press, New York, Oxford, 1999.

[21] J. Livage, O. Pelletier, P. Davidson, J. Sol–Gel Sci. Technol. 19 (2000) 275.

[22] (a) Y. Yao, T. Oka, N. Yamamoto, J. Mater. Chem. 2 (1992) 331 ;
(b) V. Petkov, P.N. Trikalitis, E.S. Bozin, S.J.L. Billinge, T. Vogt, M.G. Kanatzidis, J. Am. Chem. Soc. 124 (2002) 10157 ;
(c) O. Durupthy, N. Steunou, T. Coradin, J. Maquet, C.J. Bonhomme, J. Livage, J. Mater. Chem. 15 (2005) 1090.